Hindawi Publishing Corporation
International Journal of Antennas and Propagation
Volume 2013, Article ID 176704, 17 pages
http://dx.doi.org/10.1155/2013/176704

Research Article

Quantification of Scenario Distance within Generic WINNER Channel Model

Milan Narandžić,[1] Christian Schneider,[2] Wim Kotterman,[3] and Reiner S. Thomä[2]

[1] *Department for Power, Electronic and Communication Engineering, Faculty of Technical Sciences, Trg D. Obradovića 6, 2100 Novi Sad, Serbia*
[2] *Electronic Measurement Research Lab, Ilmenau University of Technology, PSF 100565, 98684 Ilmenau, Germany*
[3] *Digital Broadcasting Research Laboratory, Ilmenau University of Technology, PSF 100565, 98684 Ilmenau, Germany*

Correspondence should be addressed to Milan Narandžić; orange@uns.ac.rs

Received 27 July 2012; Revised 29 October 2012; Accepted 1 November 2012

Academic Editor: Ai Bo

Starting from the premise that stochastic properties of a radio environment can be abstracted by defining scenarios, a generic MIMO channel model is built by the WINNER project. The parameter space of the WINNER model is, among others, described by normal probability distributions and correlation coefficients that provide a suitable space for scenario comparison. The possibility to quantify the distance between reference scenarios and measurements enables objective comparison and classification of measurements into scenario classes. In this paper we approximate the WINNER scenarios with multivariate normal distributions and then use the mean Kullback-Leibler divergence to quantify their divergence. The results show that the WINNER scenario groups (A, B, C, and D) or propagation classes (LoS, OLoS, and NLoS) do not necessarily ensure minimum separation within the groups/classes. Instead, the following grouping minimizes intragroup distances: (i) indoor-to-outdoor and outdoor-to-indoor scenarios (A2, B4, and C4), (ii) macrocell configurations for suburban, urban, and rural scenarios (C1, C2, and D1), and (iii) indoor/hotspot/microcellular scenarios (A1, B3, and B1). The computation of the divergence between Ilmenau and Dresden measurements and WINNER scenarios confirms that the parameters of the C2 scenario are a proper reference for a large variety of urban macrocell environments.

1. Introduction

In order to maximize transmission efficiency, wireless communication systems are forced to exploit the spatial and temporal dimensions of the radio channel to the full. The design and performance analysis of such system requires the channel model to reflect all relevant propagation aspects, which imposes serious constraints on the minimal complexity of the model.

This paper concentrates on the class of geometry-based stochastic channel models (GSCMs) that offer good trade-off between complexity and performance (realism). These models deal with physical ray propagation and therefore implicitly or explicitly include the geometry of the propagation environment. The flexible structure of GSCMs enables the representation of different propagation environments by simple adjustment of model parameters, which is referred to as *generic* property. The generic models introduce abstract classes called *scenarios* that act as stochastic equivalents for many similar radio environments. As discussed in [1] these scenarios are not necessarily distinguished by the quantification of parametric space, but they represent a convenient terminology to designate typical deployment and propagation conditions. From history, it was COST207 [2] that started classifying environments based on the type of dispersion (delay spread and delay window), so some intuitive consideration of the (rather limited) parameter space was involved. But, these types of differences have (almost) never been sought later on, when defining new scenarios, especially following deployment schemes.

Nowadays we can distinguish between two major classes of generic models: COST 259/273/2100 ([3–5], resp.) and 3GPP SCM [6]/WINNER [7, 8]. The first one defines spatial regions where interacting objects become "visible,"

that is, contributing to the total received field. The second class offers an abstraction of the environment in parametric space by using delay and angular spreads, cross-polarization, shadowing, K-factor, and so forth. These generic models have been made by joint effort of many institutions; otherwise provision of parameters for different scenarios would be unattainable. Despite different model structures, significant overlap of propagation scenario definitions exists between SCM/WINNER and COST models [9].

The need for generic models follows from the ever growing concept of heterogeneous networks, requiring simultaneous representation of multiple scenarios or transitions between scenarios. For this purpose scenarios of generic models provide a uniform modeling approach and decrease the perceived complexity of handling different environments.

A reduction of the number of scenarios in generic models also reduces the necessary time and effort for design and performance evaluation of communication systems. Since every environment is specific, the classification of propagation environments into the different (reference) scenarios is not a simple task: how many classes suffice and how much divergence within a class should be tolerated? Obviously, a meaningful answer can be provided only if we have a metric to quantify the similarity between propagation environments. Providing such a metric is the main goal of this paper.

In absence of a scenario distance metric, reference scenarios are typically formed as a combination of system deployment schemes, mobility assumptions, and narrative description of environments, as illustrated in Section 2 for the WINNER reference propagation scenarios. The structure of the WINNER channel model and an approximation of its parametric space with multivariate normal distribution are given in Section 3. Section 4 describes measurement experiments used for the validation of the proposed distance metric and WINNER scenario parameters. The mean Kullback-Leibler divergence is introduced in Section 5 and is exploited to quantify the similarity between the approximated WINNER scenarios. Necessary modifications of the WINNER correlation coefficients are explained in the same section. Section 6 presents the results of measurement classification based on the introduced divergence measure, and Section 7 concludes the paper.

2. WINNER Reference Propagation Scenarios

The WINNER (Wireless World Initiative New Radio) project [10] was conducted in three phases (I, II, and +) from 2004 until 2010, with the aim to define a single ubiquitous radio access system concept, scalable and adaptable to different short range and wide area scenarios. The effects of the radio-propagation on the overall system design are abstracted by the introduction of Reference Propagation Scenarios (RPSs). RPSs are related to WINNER system-deployment schemes, being suitably selected to represent different coverage ranges: wide area (WA), metropolitan area (MA), and local area (LA), and each deployment scheme was described by as few propagation scenarios as possible. The outcome is that the WINNER scenarios cover some typical cases, without the intent to encounter all possible propagation environments.

The WINNER reference propagation scenarios [7] are determined by the aspects that have immediate impact on the radio-signal propagation:

(i) propagation environment,

  (a) LoS/NLoS condition,
  (b) limited distance range,

(ii) terminal positions (heights) with respect to environment,

(iii) mobility model (terminal speed),

(iv) carrier frequency range/bandwidth.

Due to different propagation mechanisms under LoS and NLoS conditions, they are distinguished and separately characterized in all applicable physical environments.

All WINNER reference propagation scenarios are represented by generic channel model. This model, called WINNER channel Model (WIM), has been developed within the 3GPP Spatial Channel Model (SCM) framework. By its nature, these models are representing the wideband MIMO channels in static environments for nonstationary users. The MATLAB implementations of SCM and WIM are publicly available through the project website [10]. At the end of the phase II, WIM was parameterized for 12 different scenarios, being listed in Table 1. The full set of WIM RPS parameters can be found in Sections 4.3 and 4.4 of the WINNER deliverable D1.1.2 [7]. Relations between WINNER reference propagation scenarios and WIM parameters are illustrated in Figure 1.

The characterization of the reference propagation scenarios and parametrization of the generic model are based on channel sounding results. In order to collect relevant data, a large number of measurement campaigns have been carried out during the project. However, the realization of large-scale campaigns and the subsequent processing of the results are both complex and time consuming. As a consequence, the WINNER "scenario" is formed on the basis of measurement results that are gathered by different institutions and are individually projected on the parameter set of WINNER model. These measurements were conducted in radio environments providing the best possible match with defined reference scenarios. For that purpose, the position and movement of communication terminals were chosen according to the typical usage pattern. The resulting scenario-specific model parameters sometimes also include results found in the literature, in order to come up with the most typical representatives for a targeted scenario.

3. Structure of the WINNER Channel Model

WIM is a double-directional [11] geometry-based stochastic channel model, in which a time-variable channel impulse response is constructed as a finite sum of Multi-Path Components (MPCs). The MPCs are conveniently grouped into clusters, whose positions in multidimensional space are

Table 1: WINNER reference propagation scenarios.

Scenario	Definition	LoS/NLoS	Mob. [km/h]	AP ht [m]	UE ht [m]	Distance range [m]	Coverage
A1 (In building)	Indoor small office/residential	LoS/NLoS	0–5	1–2.5	1–2.5	3–100	LA
A2	Indoor-to-outdoor	LoS/NLoS	0–5	2–5 + floor height	1-2	3–1000	LA
B1 (Hotspot)	Typical urban microcell	LoS/NLoS	0–70	Below RT (3–20)	1-2	10–5000	LA, MA
B2	Bad urban microcell	LoS/NLoS	0–70	Below RT	1-2	10–5000	MA
B3 (Hotspot)	Large indoor hall	LoS	0–5	2–6	1-2	5–100	LA
B4	Outdoor-to-indoor	LoS/NLoS	0–5	Below RT	1-2	3–1000	MA
B5a (Hotspot, Metropol)	LoS stat. feeder, rooftop to rooftop	LoS	0	Above RT	Above RT	30–8000	MA
B5b/C5b (Hotspot, Metropol)	LoS stat. feeder, street level to street level	LoS	0	3–5	3–5	20–400	MA
B5c (Hotspot, Metropol)	LoS stat. feeder, below rooftop to street level	LoS	0	Below RT, for example, 10	3–5	20–1000	MA
B5d (Hotspot, Metropol)	NLoS stat. feeder, above rooftop to street level	NLoS	0	Above RT, for example, 32	3–5	35–3000	MA
B5f	Feeder link BS $\rightarrow$ FRS. Approximately RT to RT level	LoS/OLoS/NLoS	0	RT, for example, 25	RT, for example, 15	30–1500	WA
C1 (Metropol)	Suburban	LoS/NLoS	0–120	Above RT, 10–40	1-2	30–5000	MA, WA
C2 (Metropol)	Typical urban macrocell	NLoS	0–120	Above RT, for example, 32	1-2	10–5000	MA, WA
C3	Bad urban macrocell	LoS/NLoS	0–70	Above RT	1-2	50–5000	—
C4	Outdoor-to-indoor	LoS/NLoS	0–5	Above RT	1-2 + floor height	50–5000	MA
D1 (Rural)	Rural macrocell	LoS/NLoS	0–200	Above RT, for example, 45	1-2	35–10000	WA
D2a	Moving networks: BS—MRS, rural	LoS	0–350	20–50	2.5–5	30–3000	WA
D2b	Moving networks: MRS—MS, rural	LoS/OLoS/NLoS	0–5	>2.5	1-2	3–100	WA

Table 2: Large-scale parameters of WINNER model.

LSP Name	Acronym	Power distribution
Shadow fading	SF	Around mean transmission loss
Delay spread	DS	Over delay domain
Angular spread		Over angular domain:
	ASD/ASA	(i) at Departure and Arrival
	ESD/ESA	(ii) over Azimuth and Elevation, "Azimuth/Elevation"
Narrowband K-factor	K	Betw. LoS and NLoS clusters
CROSS polar. ratio	XPR	Betw. co- and cross-polar MPCs

determined by Large-Scale Parameter (LSP) realizations. LSPs are controlling the distribution of the power (spreading) over the individual dimensions of the channel, as indicated in Table 2.

Within the modeling context LSPs are exploited to govern the evolution of the synthesized channel. The entire process of WIM parameter synthesis can be done in three hierarchy levels [9].

(1) On top level, large-scale parameters listed in Table 2 are drawn randomly from tabulated log-normal Probability Density Functions (PDFs). With the exception of XPR, all other LSPs are generated as *correlated* random variables.

(2) On the second level, cluster parameters are determined. For the sake of the simplicity this level of freedom is reduced in SCM/WIM, since all clusters share the same (scenario dependent) intra-Cluster Angular Spread (CAS).

(3) In order to further simplify cluster characterization, SCM/WIM does not deal with random placement of MPCs in delay or angular domains. Instead, the same, simple internal structure of the cluster is used and MPC parameters are calculated in a deterministic manner.

Following the given WIM approximations the LSPs become the most important for the particular scenario characterization. We would therefore ignore the lower hierarchy levels when computing a scenario divergence in Section 5.

3.1. Transformed LSP Domain. The WINNER model investigates LSP distributions and their correlations in transformed domain [6] where normal distributions for all transformed LSPs are assumed. For log-normally distributed LSPs (delay and angular spreads) the mapping $\tilde{s} = g(s) = \log_{10}(s)$ is applied (Figure 2). The remaining LSPs (SF, XPR, and K-factor) have Gaussian distributions when expressed in (dB). The WINNER tables specify marginal (per-dimension) TLSP distributions with mean and variance parameters $(\mu_i, \sigma_i)_{i=1,\ldots,k}$ and matrix of correlation coefficients $\boldsymbol{\rho} = [\rho_{i,j}]_{i=1,\ldots,k;\ j=1,\ldots,k}$. The entries of this matrix express pairwise correlations of the LSPs x_i and x_j in the form of the correlation coefficient:

$$\rho_{i,j} = \frac{\mathrm{Cov}\left[x_i, x_j\right]}{\sqrt{\mathrm{Cov}\left[x_i, x_i\right]\mathrm{Cov}\left[x_j, x_j\right]}} = \frac{\sigma_{i,j}^2}{\sigma_i \sigma_j}, \quad (1)$$

where $\sigma_{i,j} = \mathrm{Cov}[x_i, x_j] = E[(x_i - E[x_i])(x_j - E[x_j])]$. Figure 3 shows marginal distributions of delay spread in transformed domain for all WIM reference scenarios having NLoS propagation and additionally includes the maximum likelihood estimate of normal distributions for Ilmenau and Dresden measurements, which will be discussed in the following sections.

3.1.1. Multivariate Normal Distribution of TLSPs. The multivariate normal probability density function of a k-dimensional random vector $\mathbf{x} = [x_1, x_2, \ldots, x_k]^T : \mathcal{N}(\boldsymbol{\mu}, \boldsymbol{\Sigma})$ can be expressed as [12]

$$f(\mathbf{x}) = \frac{1}{(2\pi)^{k/2}|\boldsymbol{\Sigma}|^{1/2}} \exp\left(-\frac{1}{2}(\mathbf{x} - \boldsymbol{\mu})^T \boldsymbol{\Sigma}^{-1}(\mathbf{x} - \boldsymbol{\mu})\right), \quad (2)$$

where

$$\boldsymbol{\mu} = E[\mathbf{x}] \in \mathbb{R}^k \quad (3)$$

is k-dimensional mean vector and $k \times k$ covariance matrix is

$$\boldsymbol{\Sigma} = \mathrm{Cov}[\mathbf{x}, \mathbf{x}] = E\left[(\mathbf{x} - E[\mathbf{x}])(\mathbf{x} - E[\mathbf{x}])^T\right] \in \mathbb{R}^{k \times k}. \quad (4)$$

Although the structuring of the WIM TLSP distribution parameters is slightly different, they basically represent maximum-likelihood estimates of a multivariate normal (MVN) distribution parameters (3) and (4). (The random variables showing very specific dependence are not jointly normally distributed even if their marginal distributions are normal. Since only dependence between continuous WIM LSPs is expressed by the correlation coefficient (1), we assume without explicit proof that the vector of LSPs will have jointly normal distribution.) It is therefore possible to reconstruct the full covariance matrix of MVN by the following scaling:

$$\boldsymbol{\Sigma} = \boldsymbol{\Sigma}_0^{1/2} \boldsymbol{\rho} \boldsymbol{\Sigma}_0^{1/2}, \quad (5)$$

where

$$\boldsymbol{\Sigma}_0 = \mathrm{diag}\left(\sigma_1^2, \sigma_2^2, \ldots, \sigma_k^2\right) \quad (6)$$

represents the diagonal covariance matrix of the uncorrelated LSPs. Accordingly, every WINNER scenario can be abstracted with (up to) 8-dimensional normally distributed random process where relevant dimensions describe different large-scale parameters listed in Table 2. In a given case, the multivariate normal process offers a straightforward approximation of WINNER scenario since the majority of them have identical cluster structure.

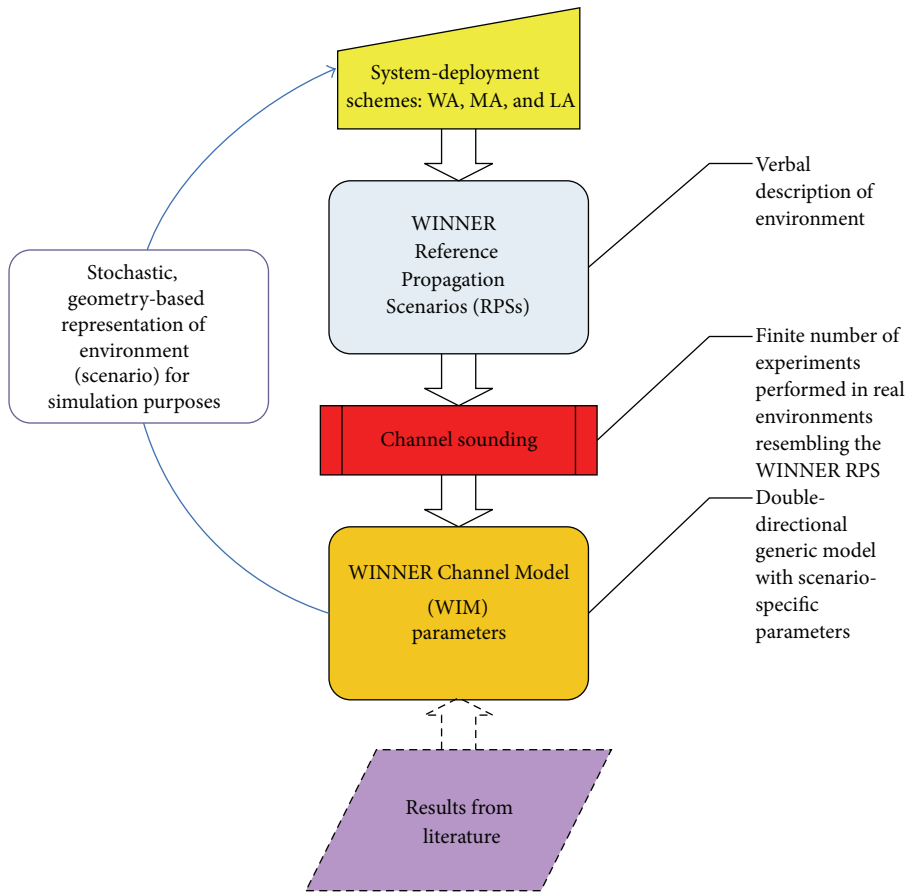

Figure 1: Genesis and representation of WINNER reference propagation scenarios [9].

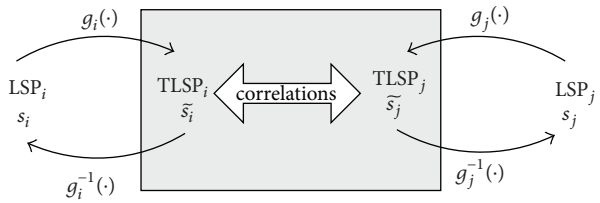

Figure 2: LSP are characterized and synthetized in transformed domain.

3.2. Terminal Separation. Although WIM describes the propagation environment implicitly within LSP parametric space, it is still using distance to govern transmission loss and spatial variations of LSP realizations.

Local stationarity region represents a larger area where multipath structure of physical propagation channel does not change significantly ("local region of stationarity" [13], "drop" [6], and "channel segment" [7]), and it is therefore characterized by a single realization from multidimensional LSP distribution. In WINNER model it is conveniently assumed that the extent of local stationarity region can be represented by the scenario-dependent constant (*decorrelation distance*) that is independent from the LSP cross-correlations.

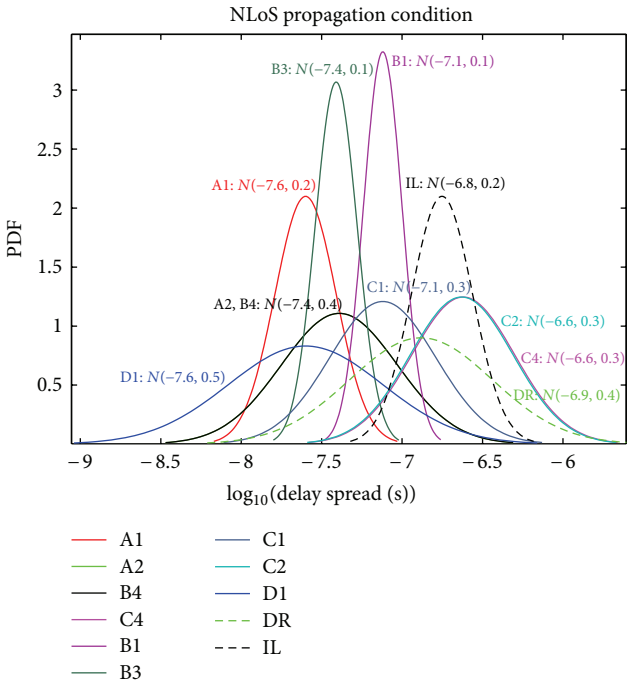

Figure 3: Delay spread PDFs in transformed domain.

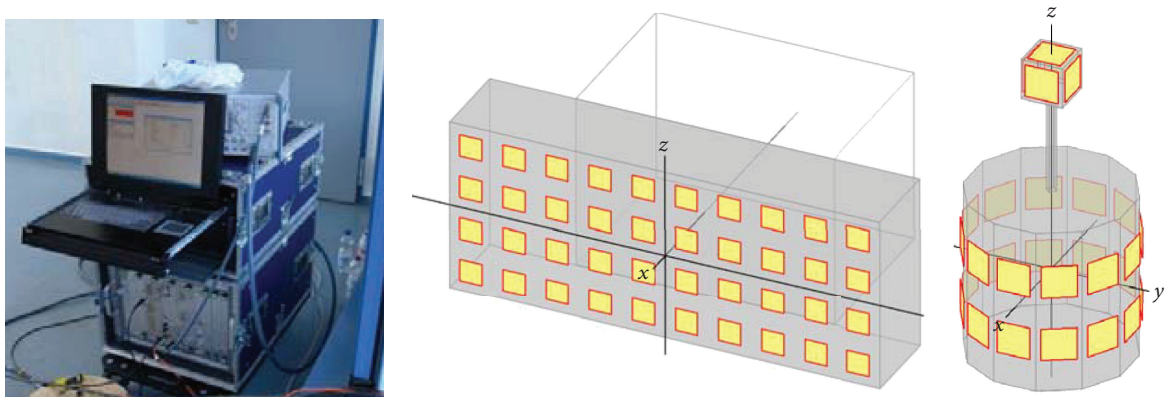

(a) (b) (c)

Figure 4: Measurement equipment: RUSK sounder (Tx) and antenna arrays—PULA8 (Tx) and SPUCA12 + MIMO-Cube (Rx).

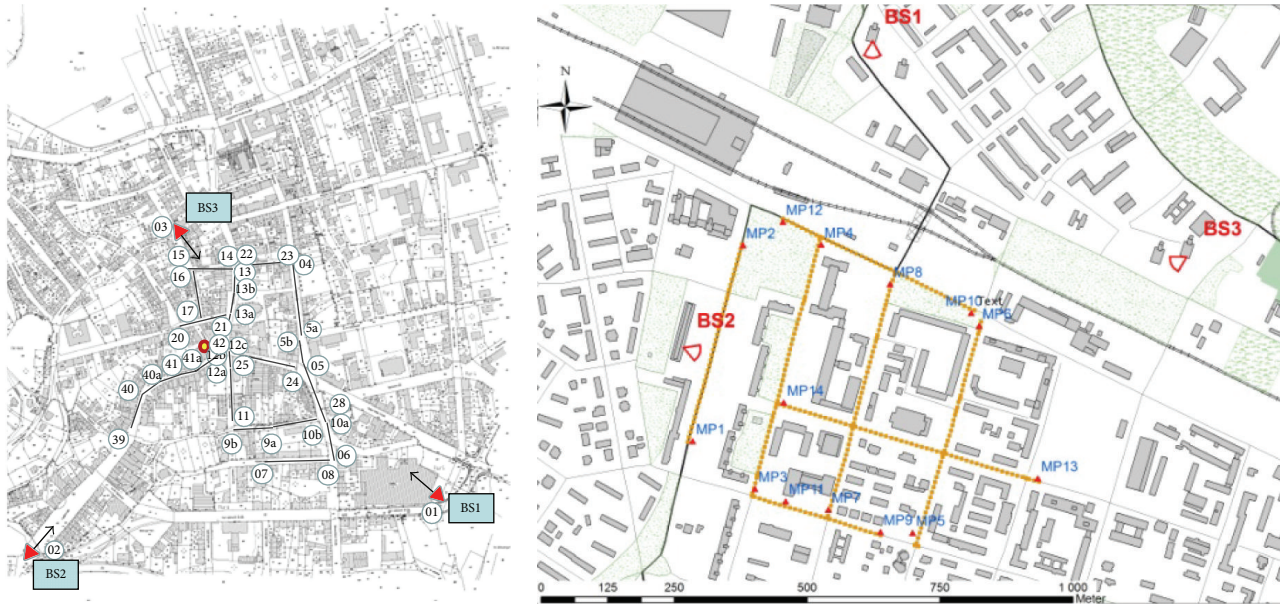

(a) (b)

Figure 5: BS locations and measurement tracks in Ilmenau and Dresden.

Both transmission loss and decorrelation distance are deterministic features in WIM. They do not impact MVN distribution of TLSPs and could be analyzed independently. Therefore, we investigate MVN process as joint model for WINNER LSP marginal distributions and cross-correlation coefficients. This representation of multidimensional channel, on the scenario scale, can be considered as a generalization of the 1D small-scale fading channel approach, where stochastic properties of instantaneous envelope are characterized by PDF.

4. Representation of Measurements in WINNER Parametric Space

The multidimensional sounding enables the investigation of the complete spatiotemporal structure of a radio channel that, additionally to the temporal delay of incoming waves, includes their angular directions at transmission and at reception as well as their polarizations. This can be achieved by the specialized estimation algorithms as RIMAX [14] when calibration data of double-polarized measurement antenna

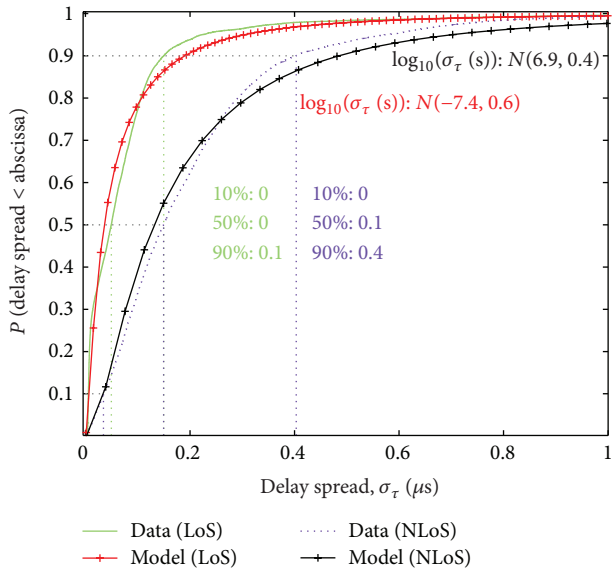

FIGURE 6: Distributions of delay spreads in Dresden measurement.

array is available [15, 16]. The multidimensional sounding is performed by dedicated RF equipment that sequentially transmits and measures channel responses between multiple antennas on transmitter and receiver sides. This approach requires high reliability of the time referencing of measurement data on both sides of radiolink, which is typically achieved by highly stable rubidium or cesium clocks.

4.1. Measurement Campaigns. In this paper data from two measurement experiments will be exploited: the first one is performed in Ilmenau, Germany, in 2008 and the second in Dresden, Germany in 2009. In the rest of the paper they will be conveniently labeled as IL and DR, respectively. Both measurements are performed with Medav RUSK channel sounder [17] at 2.53 GHz using frequency bandwidth of 100 MHz. To allow high-resolution parameter estimations of multipath structure, dedicated antenna arrays at transmit and receive sides are used, providing a total of 928 MIMO subchannels (Figure 4). The time necessary to record the responses of all wideband MIMO sub-channels, T_S, was 12.1 ms for Ilmenau and 24.2 ms for Dresden measurement. This limits the maximally allowed speed between the measurement vehicle and other interacting objects, $v \leq \lambda/2T_S$, to 17.6 km/h and 8.8 km/h, respectively ($\lambda \approx 12$ cm denotes the wavelength of the carrier). Under these conditions channels are properly sampled in space-time.

In both campaigns, three well-separated base station locations within city centers are used (Figure 5), and mobile terminal is positioned on the rooftop of the car. The same macrocell measurement setup, including the configuration of the measurement equipment, provides the proper base for comparison of Ilmenau and Dresden propagation environments. Ilmenau is a small city compared to Dresden: whereas Ilmenau is characterized by 3-4 floor buildings, Dresden has buildings with 6–8 floors. Subsequently the base station height at Dresden (~50 m) was almost doubled compared to Ilmenau (~25 m).

4.2. Estimated MVN Distribution Parameters. Data from both measurement locations is used to estimate the parameters of WINNER model. The parameters of marginal LSPs and corresponding correlation coefficients estimated from Ilmenau and Dresden measurements are given in Tables 8 and 9 together with parameters describing WINNER reference propagation scenarios. Additional details regarding Ilmenau and Dresden measurements and analysis can be found in [18, 19], respectively.

According to the description of WINNER reference propagation scenarios, both measurements should be assigned to the typical urban macrocell scenario, C2. Since both measurements are conducted after the publication of WIM-C2 parameters, they provide a proper test set for the validation of reported WIM parameters.

4.2.1. Normality of Estimated LSPs in Transformed Domain. Figure 6 shows maximum likelihood fit of the empirical delay spread CDF from Dresden measurement with WINNER-like log-normal distribution. Although this approximation seems reasonable, the null hypothesis, that collected and transformed DS samples coming from normal distribution, is rejected by both Lilliefors [20] and Jarque-Bera [21] normality tests. In contrast to the one-sample Kolmogorov-Smirnov test, these tests are suitable when parameters of null distribution are unknown and must be estimated. The normality hypothesis is also rejected for other large-scale parameters estimated from Ilmenau and Dresden data, for both LoS and NLoS conditions. Therefore the representation of measurements in WINNER parametric space can be considered as maximum-likelihood approximation of empirical multivariate distribution with MVN process.

5. Quantification of Scenario Distance

As showed in Section 3.1.1, the parameter set of WINNER model is equivalent to the parameters of the multivariate normal distribution. Therefore, all measurement projections and reference scenarios share the same parameter set and could be treated as multivariate probability distributions. This enables the introduction of a metric to quantify the divergence (distance) between different projections of measurements on the parameter set of the model, including the representatives of different reference scenarios. In order to illustrate the (dis)similarity between B3 and C2 WINNER scenarios under LoS and NLoS propagation, joint 2D PDFs of delay spread and shadow fading are presented in Figure 7. We can observe that these scenarios have differences, but some kind of similarity measure will be useful. Having in mind that we want to quantify the distance between two

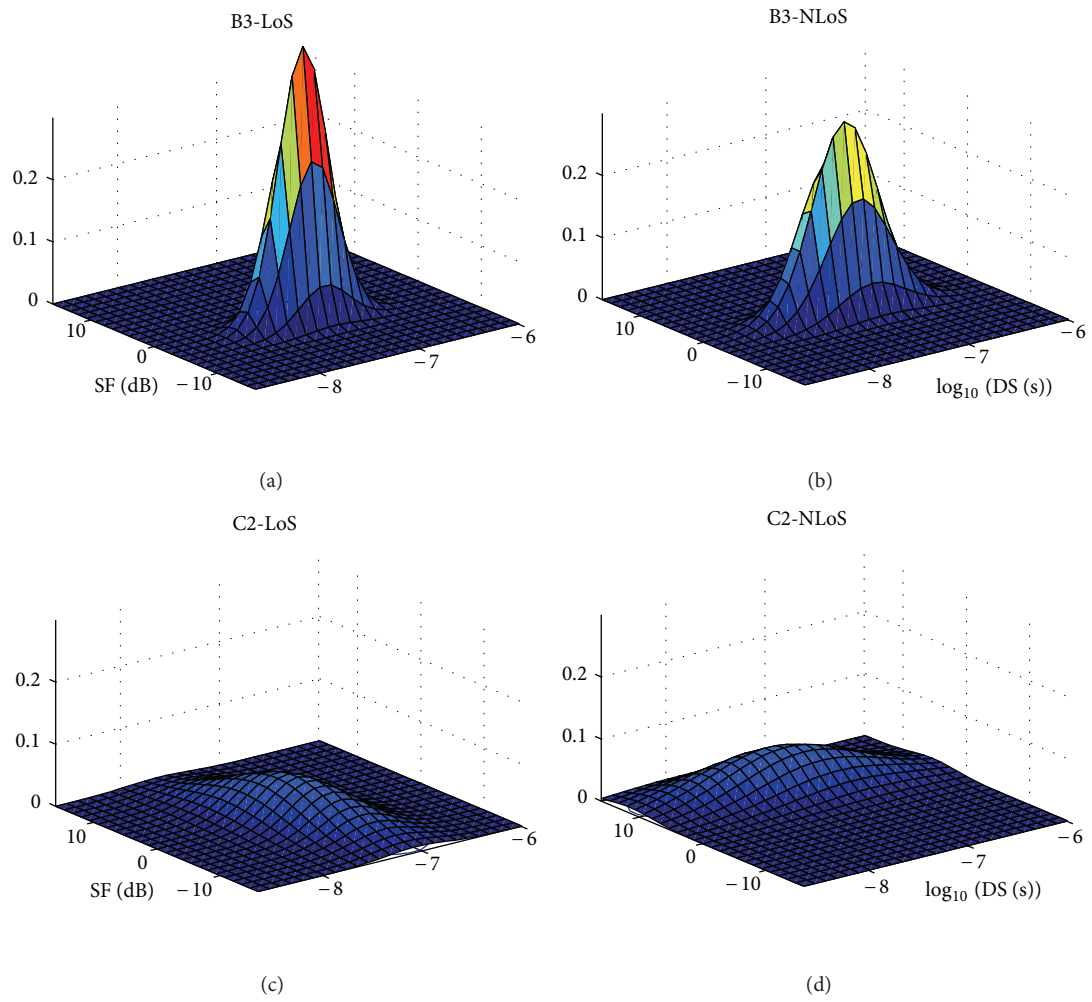

Figure 7: Comparison of joint (DS and SF) PDFs for B3 and C2 WINNER scenarios, for LoS and NLoS propagation.

distributions P and Q, it is possible to apply some form of relative entropy, for example, Kullback-Leibler (KL) divergence [22]:

$$D_{\mathrm{KL}}(P\|Q) = \int_{\mathbf{x}\in\mathbb{R}^k} p(\mathbf{x}) \log_2 \frac{p(\mathbf{x})}{q(\mathbf{x})} d\mathbf{x}, \tag{7}$$

where p and q denote the densities of P and Q. The computation of the KL divergence according to (7) would require multidimensional mapping of the $\mathbb{R}^k$ subset into two PDFs: p and q. This approach may become impractical for a large number of dimensions: in the case of WINNER it is necessary to consider up to 8 dimensions (although the XPR is not correlated with other LSPs). The marginal PDFs of K-factor are given only for scenarios with LoS propagation what reduces the dimensionality of MVN distribution for NLoS propagation for 1.

In a special case when considering divergence between two MVN distributions it is possible to construct an analytical expression that depends solely on distribution parameters. The Kullback-Leibler divergence from $\mathcal{N}_0(\mu_0, \Sigma_0)$ to $\mathcal{N}_1(\mu_1, \Sigma_1)$, for nonsingular matrices Σ_0 and $\Sigma_1 \in \mathbb{R}^{k\times k}$, is [23]

$$D_{\mathrm{KL}}(\mathcal{N}_0\|\mathcal{N}_1) = \frac{1}{2\log_e 2}\cdot\left[\log_e\left(\frac{\det(\Sigma_1)}{\det(\Sigma_0)}\right) + \mathrm{tr}\left(\Sigma_1^{-1}\Sigma_0\right) + (\mu_1-\mu_0)^{\top}\Sigma_1^{-1}(\mu_1-\mu_0) - k\right]. \tag{8}$$

This metric enables a simple comparison of reference WINNER scenarios. Therefore we found that the original form of KL metric (7) is more suitable for this particular problem than its symmetrized form, the Jansen-Shannon divergence [24]. Since KL divergence is not symmetric, it is necessary to define some other symmetrized extension to obtain proper distance metric. We propose to use mean KL divergence:

$$D_{\overline{\mathrm{KL}}}(P\|Q) = \frac{1}{2}\left[D_{\mathrm{KL}}(P\|Q) + D_{\mathrm{KL}}(Q\|P)\right]. \tag{9}$$

5.1. Negative Definite Covariance Matrices. In some cases negative or complex values are obtained for KL divergence, indicating that the matrix of correlation coefficients ($\boldsymbol{\rho}$) is not positive semidefinite, that is, $\boldsymbol{\rho} < 0$. The problem is manifesting only for scenarios with resolved elevation angles (Table 3) where the dimensionality of the MVN distribution is increased from 6 (LoS)/5 (NLoS) to 7/6 or 8/7. The problem is, however, not related to the number of dimensions or elevation parameters themselves since simple removal of elevation dimension(s) does not resolve it. This means that correlation coefficients between WINNER LSPs analyzed jointly do not form a proper correlation matrix (CM)—not even without elevations.

It is observed that the number of decimal places used for representation of CM elements cannot be arbitrarily reduced since the resulting matrix may become negative definite. Since individual coefficients in WINNER parameter tables are expressed using only one decimal place, it is possible that this lack of precision causes negative definite CM for scenarios with an increased number of dimensions.

In order to enable the comparison of problematic scenarios their correlation coefficients have to be slightly modified to form positive definite CM. The "real" correlation matrix is computed using alternate projections method (APM) [25, 26]. For a given symmetric matrix $\boldsymbol{\rho} \in \mathbb{R}^{k \times k}$ this method finds the nearest correlation matrix $\widehat{\boldsymbol{\rho}}$, that is, (semi) definite, and has units along the main diagonal. The solution is found in the intersection of the following sets of symmetric matrices $S = \{Y = Y^T \in \mathbb{R}^{k \times k} \mid Y \geq 0\}$ and $U = \{Y = Y^T \in \mathbb{R}^{k \times k} \mid y_{ii} = 1,\ i = 1, \ldots, k\}$. The iterative procedure in nth step applies updated Dykstra's correction ΔS_{n-1} and subsequently projects intermediate result to both matrix sets, using projections P_S and P_U:

$$
\begin{aligned}
&\Delta \mathbf{S}_0 = 0, \qquad \mathbf{Y}_0 = \boldsymbol{\rho}, \qquad n = 0 \\
&\text{do} \\
&\quad n = n + 1 \\
&\quad \mathbf{R}_n = \mathbf{Y}_{n-1} - \Delta \mathbf{S}_{n-1} \\
&\quad \mathbf{X}_n = P_S\left(\mathbf{R}_n\right) \\
&\quad \Delta \mathbf{S}_{n-1} = \mathbf{X}_n - \mathbf{R}_n \\
&\quad \mathbf{Y}_n = P_U\left(\mathbf{X}_n\right) \\
&\text{while } \left\|\mathbf{Y}_n - \mathbf{Y}_{n-1}\right\|_F < tol.
\end{aligned}
\tag{10}
$$

The projection P_S replaces all negative eigenvalues of the matrix with a small positive constant ϵ, and P_U forces ones along the main diagonal. The procedure stops when Frobenius distance $\|\cdot\|_F$ between Y_n projections from two consecutive iterations drops below a predefined tolerance tol. Note, however, that the small tolerance parameter does not insure that Frobenius distance (FD) from the original matrix is equally small.

The positive definite approximation $\widehat{\boldsymbol{\rho}}$ obtained by APM will depend on the selected parameters ϵ and tol [27]: for $tol = 10^{-10}$, the effect of eigenvalue ϵ on Frobenius distance FD $= \|\boldsymbol{\rho} - \widehat{\boldsymbol{\rho}}\|_F$ is illustrated in Table 3. The results show that FD decreases when a smaller value of ϵ is used to substitute originally negative eigenvalues. However, the selection of small ϵ will proportionally increase the eigenvalues and coefficients of the inverse correlation matrix, $\widehat{\boldsymbol{\rho}}^{-1}$. This will consequently increase the KL divergence (7) to all other scenarios. As a compromise, the new WINNER correlation coefficients corresponding to positive definite matrix are recomputed for $\epsilon = 10^{-2}$ and $tol = 10^{-10}$ and given in Table 9. The maximal absolute modification of original correlation coefficients per scenario, $\max\{|\Delta\rho_{i,j}|\}$, where $\Delta\rho_{i,j} = \rho_{i,j} - \widehat{\rho}_{i,j}$, is given in Table 3. The highest absolute correction $\Delta\rho = 0.13$ is applied to C2-NLoS scenario.

The minimum number of decimal places required to keep $\widehat{\boldsymbol{\rho}}$ positive definite is determined for different values of ϵ and listed in Table 3. The results show that smaller Frobenius distance requires higher precision for saving coefficients. For $\epsilon = 10^{-2}$ two decimal places are sufficient to express correlation coefficients for all scenarios (Table 9).

5.2. Mean KL Divergence. In order to enable comparisons between LoS and NLoS scenarios where K-factor is missing under NLoS, as well as other scenarios where certain parameters (dimensions) are missing, the reduction of dimensionality was necessary: only those dimensions existing in both scenarios are used to calculate the mean KL divergence. This means that scenarios with lower number of resolved dimensions could exhibit more similarity as a consequence of incomplete representation. A fair comparison would be possible only if all scenarios have the same number of dimensions. The respective mean KL divergences between all WINNER scenarios, including Ilmenau and Dresden measurements, are given in Table 4 (for WINNER scenarios that give two sets of LoS parameters, mean KL distances are computed for LoS parameters before breakpoint distance of transmission loss).

In order to simplify the analysis of obtained results, for each (scenario, propagation) combination the closest match is found and listed in Table 5. Divergences within the same WINNER scenario group, or having same propagation conditions, are not minimum as may have been expected. Table 5 shows that only 5 among 16 WINNER scenarios have the closest match within the same WINNER group (A, B, C, and D). This comes as consequence of subjective classification of similar environments, without previously introduced metric. The minimum distances from Table 5, $D_{\overline{\mathrm{KL}}} = 0.1$, confirm some expectations: B4-NLoS (outdoor-to-indoor) is closest to A2-NLoS (indoor-to-outdoor) because these are reciprocal scenarios. Also, microcell and macrocell versions of outdoor-to-indoor (B4 and C4) are the closest although not belonging to the same group. Mean KL divergences from Table 5 suggest that there is a better way to group available scenarios.

The average distances between all scenarios from one WINNER group to all scenarios in the other groups are given in Table 6. If all groups gather the most similar scenarios, an average distance between any two groups will be higher than the average distance within a single group. From Table 6 we can see that this applies to groups A and D, which

Table 3: Frobenius distance (FD) between empirical corr. matrix ρ and its positive definite approximation $\widehat{\rho}$, the required number of decimal places (DP) in $\widehat{\rho}$, and maximal correction of original correlation coefficients $\max\{|\Delta\rho_{i,j}|\}$, as functions of the substituting eigenvalue ϵ in APM for $tol = 10^{-10}$.

	ϵ	10^{-1}			10^{-2}			10^{-3}			10^{-6}		
Scenario	Propagation	$\|\cdot\|_F$	DP	$\max(\|\Delta\rho\|)$	$\|\cdot\|_F$	DP	$\max(\|\Delta\rho\|)$	$\|\cdot\|_F$	DP	$\max(\|\Delta\rho\|)$	$\|\cdot\|_F$	DP	$\max(\|\Delta\rho\|)$
A1	LoS	0.245	1	0.1	0.123	2	0.04	0.108	2	0.03	0.108	2	0.03
B4	NLoS	0.316	1	0.1	0.241	2	0.1	0.227	3	0.091	0.226	4	0.091
B1	LoS	0.374	1	0.1	0.269	2	0.09	0.257	3	0.085	0.255	3	0.085
B1	NLoS	0.2	1	0.1	0.066	2	0.02	0.056	3	0.019	0.055	3	0.019
C1	LoS	0.346	1	0.1	0.203	2	0.07	0.191	3	0.065	0.19	4	0.064
C1	OLoS	0.346	1	0.1	0.203	2	0.07	0.191	3	0.065	0.19	4	0.064
C1	NLoS	0.245	1	0.1	0.245	1	0.1	0.245	1	0.1	0.245	1	0.1
C2	LoS	0.374	1	0.1	0.193	2	0.06	0.174	3	0.058	0.173	6	0.058
C2	OLoS	0.374	1	0.1	0.193	2	0.06	0.174	3	0.058	0.173	6	0.058
C2	NLoS	0.548	1	0.2	0.338	2	0.13	0.333	3	0.129	0.332	5	0.129
DR	LoS	0.168	1	0.048	0.168	1	0.048	0.168	1	0.048	0.168	1	0.048
DR	NLoS	0.116	1	0.046	0.116	1	0.046	0.116	1	0.046	0.116	1	0.046
IL	LoS	0.133	1	0.043	0.133	1	0.043	0.133	1	0.043	0.133	1	0.043
IL	NLoS	0.144	1	0.047	0.144	1	0.047	0.144	1	0.047	0.144	1	0.047

Table 4: Mean KL divergence between WINNER scenarios and Ilmenau and Dresden measurements.

Scen.		A1	A1	A2	B1	B1	B3	B3	B4	C1	C1	C2	C2	C4	D1	D1	D2a	IL	IL	
	Prop.	LoS	NLoS	NLoS	LoS	NLoS	LoS	NLoS	NLoS	LoS	NLoS	LoS	NLoS	NLoS	LoS	NLoS	LoS	LoS	NLoS	LoS
A1	NLoS	19.6																		
A2	NLoS	11.0	15.4																	
B1	LoS	78.1	44.5	57.1																
B1	NLoS	52.3	51.1	27.0	20.6															
B3	LoS	14.1	8.3	21.7	23.6	15.4														
B3	NLoS	12.3	9.9	32.9	16.2	10.1	5.4													
B4	NLoS	45.2	26.8	0.1	138.5	67.1	21.1	31.5												
C1	LoS	120.9	119.2	60.7	101.6	57.4	33.1	15.5	170.8											
C1	NLoS	224.2	262.4	29.4	86.4	98.3	17.7	9.8	280.1	54.7										
C2	LoS	55.5	41.7	27.8	48.6	55.5	23.2	10.1	72.1	23.5	103.4									
C2	NLoS	117.1	134.3	50.3	121.5	141.7	40.3	20.7	163.4	28.9	33.2	54.2								
C4	NLoS	36.4	41.3	11.4	56.1	31.5	49.4	49.5	9.8	55.3	26.8	31.1	38.5							
D1	LoS	25.1	35.8	29.5	14.2	44.2	28.2	31.5	27.0	5.9	14.1	12.9	19.1	31.2						
D1	NLoS	14.3	14.4	19.9	11.2	23.9	11.5	11.4	17.5	14.6	4.8	5.6	11.5	23.7	6.7					
D2a	LoS	15.6	18.8	30.1	6.1	11.2	13.6	9.7	25.9	7.4	8.7	9.9	15.9	31.7	6.7	5.4				
IL	LoS	84.6	64.8	149.9	51.8	45.9	49.4	24.9	145.2	32.5	23.4	35.7	16.9	130.1	55.9	24.8	36.1			
IL	NLoS	87.3	74.1	116.9	105.5	53.7	46.7	26.2	154.0	25.8	25.6	36.4	15.3	89.7	41.8	24.4	22.8	2.8		
DR	LoS	96.6	94.3	128.9	43.8	49.7	44.0	22.5	130.4	11.6	20.3	23.9	16.0	128.9	14.0	23.0	12.7	38.3	32.0	
DR	NLoS	119.2	104.8	140.8	48.2	48.8	45.1	24.4	142.3	8.6	22.0	27.4	11.0	126.9	16.5	25.2	14.4	30.1	22.8	2.7

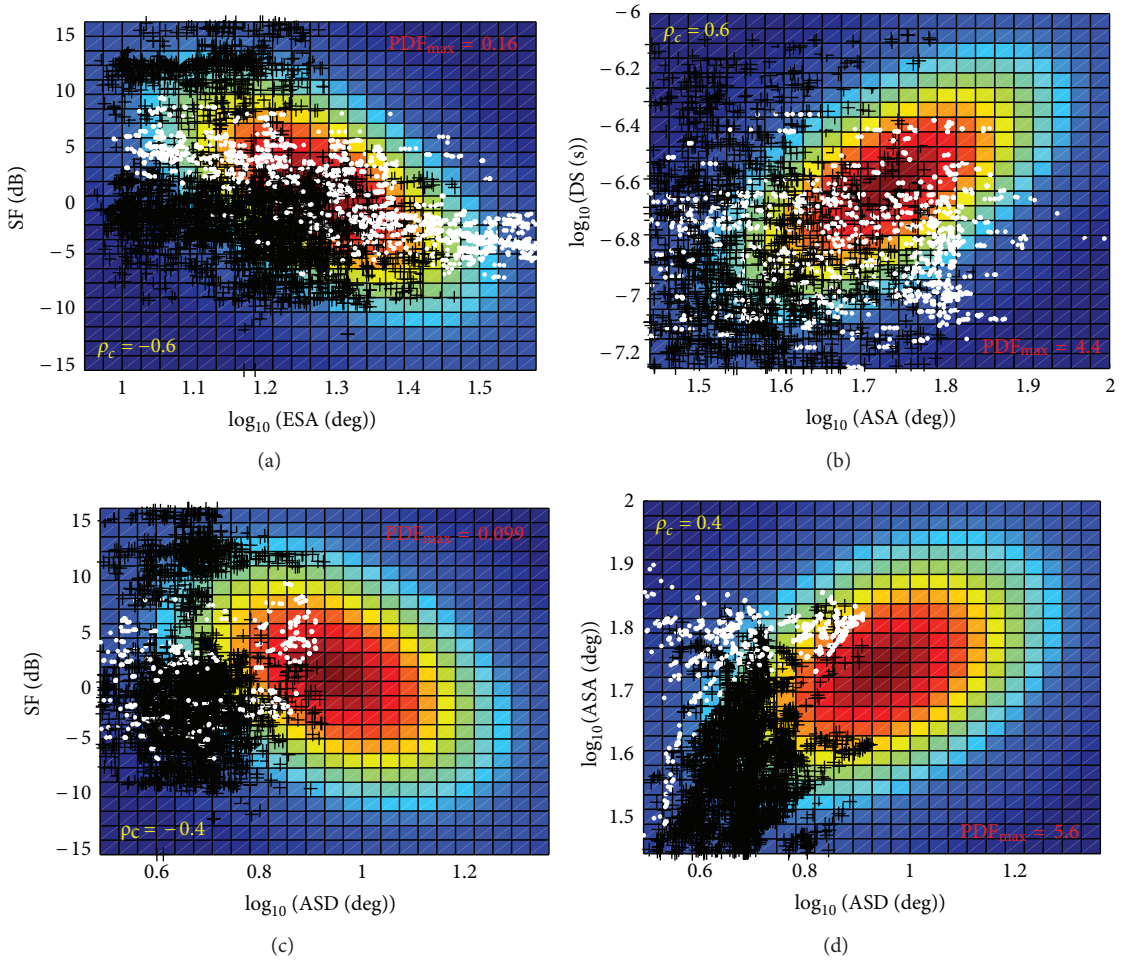

FIGURE 8: Comparison of joint WINNER C2 2D PDFs with the LSP realizations from Ilmenau (black pluses) and Dresden (white dots), for NLoS propagation.

are, according to average intergroup distance, closest to themselves. This indicates that subjective WINNER grouping can be partially supported by mean KL distance. However, the deviations are observable for groups B and C where other groups appear to be closer (at a lower average distance) than other scenarios from the same group. This situation is possibly caused by inappropriate assignment of distant scenarios, outdoor-to-indoor microcell scenario B4-NLoS and suburban C1-NLoS, to the corresponding groups.

An inspection of Table 3 reveals that the majority of scenarios with increased dimensionality (resolved elevations) come from groups B and C. This means that larger intra-group distance may appear due to increased dimensionality. Additionally, their correlation matrices have been modified by APM method, so that the parameter ϵ impacts the absolute value of the mean KL distance. The joint effect of these phenomena is illustrated by mean KL distances along the main diagonal of Table 6: they are proportional to the number of modified group members that are listed in Table 3: $\#_D = 0$, $\#_A = 1$, $\#_B = 3$, $\#_C = 6$.

TABLE 5: Closest (scenario, propagation) pairs according to mean KL divergence.

Scen.1	Prop.1	Scen.2	Prop.2	$D_{\overline{KL}}$
A1	LoS	A2	NLoS	11.0
A1	NLoS	B3	LoS	8.3
A2	NLoS	B4	NLoS	0.1
B1	LoS	D2a	LoS	6.1
B1	NLoS	B3	NLoS	10.1
B3	LoS	B3	NLoS	5.4
B3	NLoS	B3	LoS	5.4
B4	NLoS	A2	NLoS	0.1
C1	LoS	D1	LoS	5.9
C1	NLoS	D1	NLoS	4.8
C2	LoS	D1	NLoS	5.6
C2	NLoS	DR	NLoS	11.0
C4	NLoS	B4	NLoS	9.8
D1	LoS	C1	LoS	5.9
D1	NLoS	C1	NLoS	4.8
D2a	LoS	D1	NLoS	5.4
IL	LoS	IL	NLoS	2.8
IL	NLoS	IL	LoS	2.8
DR	LoS	DR	NLoS	2.7
DR	NLoS	DR	LoS	2.7

Table 6: Average distance between WINNER scenario groups: A, B, C, and D.

	A	B	C	D
A	15.3			
B	32.1	35.0		
C	88.8	70.6	45.0	
D	22.6	19.1	14.5	6.3

Table 7: Average distance between WINNER LoS and NLoS propagation conditions.

	LoS	NLoS
LoS	31.8	
NLoS	42.1	50.9

For 6 out of 16 (scenario, propagation) pairs the best match has the opposite propagation condition (LoS, instead of NLoS, and vice versa), indicating that WINNER LoS and NLoS parameters do not form disjunctive sets (Table 5). Calculation of the mean distance between all LoS and NLoS scenarios in Table 7 shows that lower average distance can be expected between scenarios having LoS propagation condition (they are more similar than different scenarios with NLoS propagation).

6. Classification of Measurements

The same criterion, KL divergence, can be applied to classify measurements as well. For this purpose even empirical distributions of LSPs can be used since KL metric (7) supports that. However, the extraction of the corresponding WINNER parameters simplifies the comparison since analytical expression (8) can be applied. Therefore we use the latter approach to compare Ilmenau and Dresden measurements with other WINNER scenarios.

Since both measurements have been performed in urban environments with macrocell setup (antennas were elevated above rooftops), it is expected that the closest scenario will be WINNER C2, which represents typical urban macrocells. These expectations are met for Ilmenau measurements, where WINNER C2-NLoS is the closest scenario for both LoS and NLoS conditions, with minimal distances $D_{\overline{\mathrm{KL}}} = 16.9$ and $D_{\overline{\mathrm{KL}}} = 15.3$ (Table 4). In the case of Dresden measurements minimal mean KL divergences (8.6 and 11.6) indicate that the closest WIM scenario is C1-LoS, for both LoS and NLoS propagation conditions. This resemblance of Dresden measurements to suburban propagation (WINNER C1) may come from dominant height of BS positions with respect to environment.

Figure 8 shows the 2D PDFs of the reference WINNER C2-NLoS scenario together with joint LSP realizations from Ilmenau and Dresden measurements. For the NLoS propagation condition Ilmenau and Dresden measurements are quite close to C2: C2-NLoS is the best match for Ilmenau-NLoS ($D_{\overline{\mathrm{KL}}} = 16.3$) and the second best match for Dresden-NLoS data ($D_{\overline{\mathrm{KL}}} = 11$). Additionally, among all results presented in Table 4 the closest match of WIM C2-NLoS is just Dresden-NLoS (row showed in red).

For LoS conditions, distances from WINNER C2 and Ilmenau and Dresden measurements are larger (35.7 and 23.9) which classifies Ilmenau-LoS to C2-NLoS ($D_{\overline{\mathrm{KL}}} = 16.9$) and Dresden-LoS into C1-LoS ($D_{\overline{\mathrm{KL}}} = 11.6$). Table 5 shows the increased similarity between LoS and NLoS propagation conditions in Ilmenau and Dresden measurements. This occurs also for WINNER B3, while other WINNER scenarios do not show this property. One possible interpretation comes from the data segmentation into LoS and NLoS classes: the actual propagation conditions for the LoS or NLoS-labeled data may actually correspond to, for example, obstructed line of sight (OLoS). The previous analysis demonstrates that mean KL divergence, additionally to the comparison of different measurements, enables the quantification of complex relations between different data segments of the same measurement, as long as they use the same LSP space representation.

The mean KL distances between Ilmenau and Dresden measurements (38.3-LoS and 22.8-NLoS) are higher than corresponding distances from these measurements to the reference WINNER-C2 scenario. This confirms that WINNER C2 parameters provide appropriate representation for a wide class of urban macro-cell environments.

7. Conclusions

The paper presents the scenario concept of WINNER and proposes its abstraction to a multivariate normal distribution of large-scale parameters. Disregarding transmission loss and decorrelation distance removes the spatial extent from scenario definitions.

The generic property of the model is exploited to compare the large-scale parameters that describe different scenarios. For this purpose, a symmetrized extension of the Kullback-Leibler divergence is proposed. This enables the comparison of parameters between reference scenarios and measurements, as well as a direct comparison of empirical LSP distributions (measured or synthesized by channel model). The given approach can be also applied to other generic stochastic models if appropriate metrics are chosen that reflect models' specifics.

The presented results indicate that, according to the mean Kullback-Leibler divergence, WINNER scenario groups or propagation classes do not ensure the minimum separation within the group/class. It appears that other criteria, for example, coverage range, were more significant for the WINNER taxonomy. Judged from the mean Kullback-Leibler divergence large similarity exists between the indoor-to-outdoor and outdoor-to-indoor scenarios (A2, B4, and C4), between macro-cell configurations for suburban, urban, and rural scenarios (C1, C2, and D1), and between the indoor/hotspot/microcellular scenarios (A1, B3, and B1).

It is demonstrated that the results of measurements could be associated with the closest WINNER scenario. As expected, typical urban macro-cell scenario C2 was the one closest to the Ilmenau measurements. For the Dresden

Table 8: LSP marginal PDF parameters.

	Scen.	A1	A1	A2	B4	C4	B1	B1	B3	B3	C1	C1	C2	C2	D1	D1	D2a	DR	DR	IL	IL
LSP	Prop.	LoS	NLoS	NLoS	NLoS	NLoS	LoS	NLoS	LoS	NLoS	LoS	NLoS	LoS	NLoS	LoS	NLoS	LoS	LoS	NLoS	LoS	NLoS
DS	μ	−7.4	−7.6	−7.4	−7.4	−6.6	−7.4	−7.1	−7.5	−7.4	−7.2	−7.1	−7.4	−6.6	−7.8	−7.6	−7.4	−7.4	−6.9	−6.9	−6.8
DS	σ	0.3	0.2	0.4	0.4	0.3	0.3	0.1	0.1	0.1	0.5	0.3	0.6	0.3	0.6	0.5	0.2	0.6	0.4	0.2	0.2
ASD	μ	1.6	1.7	1.8	1.8	1.8	0.4	1.2	1.2	1.1	0.8	0.9	1.0	0.9	0.8	1.0	0.7	0.7	0.7	0.2	0.4
ASD	σ	0.3	0.2	0.2	0.2	0.2	0.4	0.2	0.2	0.2	0.1	0.4	0.3	0.2	0.2	0.5	0.3	0.1	0.1	0.3	0.4
ASA	μ	1.6	1.7	1.3	1.3	1.3	1.4	1.6	1.6	1.7	1.5	1.6	1.7	1.7	1.2	1.5	1.5	1.5	1.6	1.6	1.6
ASA	σ	0.3	0.1	0.4	0.4	0.4	0.2	0.2	0.2	0.1	0.2	0.3	0.2	0.1	0.2	0.3	0.2	0.1	0.1	0.2	0.2
ESD	μ	0.9	1.1	N/A	0.9	N/A	0.4	0.6	N/A	N/A	0.7	0.9	0.7	0.9	N/A	N/A	N/A	N/A	N/A	N/A	N/A
ESD	σ	0.3	0.2	N/A	0.3	N/A	0.2	0.2	N/A	N/A	0.2	0.2	0.2	0.2	N/A	N/A	N/A	N/A	N/A	N/A	N/A
ESA	μ	0.9	1.1	N/A	1.0	N/A	0.6	0.9	N/A	N/A	1.1	1.0	0.9	1.3	N/A	N/A	N/A	1.2	1.2	1.3	1.3
ESA	σ	0.3	0.2	N/A	0.4	N/A	0.2	0.2	N/A	N/A	0.2	0.2	0.2	0.2	N/A	N/A	N/A	0.1	0.1	0.2	0.2
SF	μ	0.0	0.0	0.0	0.0	0.0	0.0	0.0	0.0	0.0	0.0	0.0	0.0	0.0	0.0	0.0	0.0	0.0	0.0	−0.0	0.0
SF	σ	3.0	4.0	7.0	7.0	7.0	3.0	4.0	3.0	4.0	4.0	8.0	4.0	8.0	4.0	8.0	4.0	8.3	5.3	4.0	3.6
K	μ	7.0	N/A	N/A	N/A	N/A	9.0	N/A	2.0	N/A	9.0	N/A	7.0	N/A	7.0	N/A	7.0	9.8	N/A	5.9	N/A
K	σ	6.0	N/A	N/A	N/A	N/A	6.0	N/A	3.0	N/A	7.0	N/A	3.0	N/A	6.0	N/A	6.0	7.8	N/A	7.1	N/A
XPR	μ	11.0	10.0	9.0	9.0	9.0	9.0	8.0	9.0	6.0	8.0	4.0	8.0	7.0	12.0	7.0	12.0	9.7	7.0	7.3	6.2
XPR	σ	4.0	4.0	11.0	11.0	11.0	3.0	3.0	4.0	3.0	4.0	3.0	4.0	3.0	8.0	4.0	8.0	3.6	4.1	1.2	2.2

Table 9: LSP correlation coefficients.

		LSP1	DS	DS	DS	DS	DS	DS	ASD	ASD	ASD	ASD	ASD	ASA	ASA	ASA	ASA	ESD	ESD	ESD	ESA	ESA	SF
Scen.	Prop.	LSP2	ASD	ASA	ESD	ESA	SF	K	ASA	ESD	ESA	SF	K	ESD	ESA	SF	K	ESA	SF	K	SF	K	K
A1	LoS	ρ	0.7	0.8	0.5	0.7	−0.6	−0.6	0.6	0.5	0.0	−0.5	−0.6	0.0	0.5	−0.5	−0.6	0.4	−0.4	0.0	0.0	0.0	0.4
A1	LoS	$\hat{\rho}$	0.67	0.82	0.52	0.66	−0.58	−0.59		0.48	0.03	−0.52	−0.61	0.01	0.48	−0.49	−0.60	0.38	−0.39	0.00	−0.02	−0.01	0.40
A1	NLoS	ρ	−0.1	0.3	−0.6	0.0	−0.5	N/A	−0.3	0.5	0.0	0.0	N/A	0.0	0.5	−0.4	N/A	0.5	0.0	N/A	0.0	N/A	N/A
A2	NLoS	ρ	0.4	0.4	N/A	N/A	−0.5	N/A	0.0	N/A	N/A	0.0	N/A	N/A	N/A	0.2	N/A	N/A	N/A	N/A	N/A	N/A	N/A
B1	LoS	ρ	0.5	0.8	−0.5	0.0	−0.4	−0.7	0.4	0.5	0.5	−0.5	−0.3	0.0	0.0	−0.5	−0.3	0.0	0.0	0.0	0.0	0.0	0.5
B1	LoS	$\hat{\rho}$	0.41	0.74	−0.41	0.03	−0.43	−0.65	0.44	0.44	0.48	−0.48	−0.33	−0.04	−0.01	−0.48	−0.32	0.02	−0.02	0.04	−0.01	0.01	0.49
B1	NLoS	ρ	0.2	0.4	−0.5	0.0	−0.7	N/A	0.1	0.5	0.5	0.0	N/A	0.0	0.0	−0.4	N/A	0.0	0.0	N/A	0.0	N/A	N/A
B1	NLoS	$\hat{\rho}$	0.18	0.40	−0.48	0.01	−0.68	N/A	0.10	0.48	0.49	−0.01	N/A	−0.00	−0.00	−0.40	N/A	0.01	0.01	N/A	0.01	N/A	N/A
B3	LoS	ρ	−0.3	−0.4	N/A	N/A	−0.1	−0.3	0.3	N/A	N/A	0.3	0.2	N/A	N/A	−0.4	−0.1	N/A	N/A	N/A	N/A	N/A	0.6
B3	NLoS	ρ	−0.1	0.0	N/A	N/A	−0.2	N/A	−0.3	N/A	N/A	−0.3	N/A	N/A	N/A	0.2	N/A	N/A	N/A	N/A	N/A	N/A	N/A
B4	NLoS	ρ	0.4	0.4	−0.6	0.0	−0.5	N/A	0.0	0.5	0.0	0.0	N/A	0.0	0.5	0.2	N/A	0.5	0.0	N/A	0.0	N/A	N/A
B4	NLoS	$\hat{\rho}$	0.33	0.37	−0.50	−0.03	−0.45	N/A	0.02	0.43	0.02	−0.03	N/A	−0.03	0.51	0.19	N/A	0.48	0.04	N/A	−0.01	N/A	N/A
C1	LoS	ρ	0.2	0.8	−0.5	0.0	−0.6	−0.2	0.1	0.5	0.0	−0.5	0.2	0.0	0.4	−0.5	−0.2	0.0	0.0	0.0	−0.8	0.0	0.0
C1	LoS	$\hat{\rho}$	0.20	0.75	−0.46	0.06	−0.53	−0.19	0.10	0.50	0.00	−0.50	0.20	−0.02	0.36	−0.54	−0.20	0.03	0.03	0.00	−0.75	0.00	0.00
C1	NLoS	ρ	0.3	0.7	−0.5	0.0	−0.4	N/A	0.3	0.5	−0.4	−0.4	N/A	0.0	0.0	−0.3	N/A	0.0	0.0	N/A	−0.8	N/A	N/A
C1	NLoS	$\hat{\rho}$	0.3	0.7	−0.5	−0.0	−0.4	N/A	0.3	0.5	−0.3	−0.3	N/A	−0.0	0.0	−0.3	N/A	−0.0	−0.0	N/A	−0.7	N/A	N/A
C2	LoS	ρ	0.4	0.8	−0.5	0.0	−0.4	−0.4	0.3	0.5	0.0	−0.5	0.1	0.0	0.4	−0.5	−0.2	0.0	0.0	0.0	−0.8	0.0	0.3
C2	LoS	$\hat{\rho}$	0.35	0.74	−0.44	0.01	−0.41	−0.37	0.33	0.46	0.01	−0.47	0.08	−0.04	0.39	−0.50	−0.22	0.00	−0.02	0.02	−0.77	−0.01	0.29
C2	NLoS	ρ	0.4	0.6	−0.5	0.0	−0.4	N/A	0.4	0.5	−0.4	−0.6	N/A	0.0	0.0	−0.3	N/A	0.0	0.0	N/A	−0.8	N/A	N/A
C2	NLoS	$\hat{\rho}$	0.38	0.60	−0.49	−0.02	−0.42	N/A	0.40	0.45	−0.28	−0.47	N/A	0.00	−0.00	−0.30	N/A	−0.05	−0.05	N/A	−0.67	N/A	N/A
C4	NLoS	ρ	0.4	0.4	N/A	N/A	−0.5	N/A	0.0	N/A	N/A	0.0	N/A	N/A	N/A	0.2	N/A	N/A	N/A	N/A	N/A	N/A	N/A
D1	LoS	ρ	−0.1	0.2	N/A	N/A	−0.5	0.0	−0.3	N/A	N/A	0.2	0.0	N/A	N/A	−0.2	0.1	N/A	N/A	N/A	N/A	N/A	0.0
D1	NLoS	ρ	−0.4	0.1	N/A	N/A	−0.5	N/A	−0.2	N/A	N/A	0.6	N/A	N/A	N/A	0.1	N/A	N/A	N/A	N/A	N/A	N/A	N/A
D2a	LoS	ρ	−0.1	0.2	N/A	N/A	−0.5	0.0	−0.3	N/A	N/A	0.2	0.0	N/A	N/A	−0.2	0.1	N/A	N/A	N/A	N/A	N/A	0.0
DR	LoS	ρ	−0.07	−0.03	N/A	0.06	−0.62	−0.65	0.42	N/A	0.08	−0.08	−0.06	N/A	0.25	−0.13	−0.10	N/A	N/A	N/A	−0.43	−0.27	0.73
DR	LoS	$\hat{\rho}$	−0.1	−0.0	N/A	0.1	−0.6	−0.7	0.4	N/A	0.1	−0.1	−0.1	N/A	0.3	−0.1	−0.1	N/A	N/A	N/A	−0.4	−0.3	0.7
DR	NLoS	ρ	−0.11	−0.21	N/A	−0.29	−0.49	N/A	0.40	N/A	0.05	0.06	N/A	N/A	0.27	0.12	N/A	N/A	N/A	N/A	−0.26	N/A	N/A
DR	NLoS	$\hat{\rho}$	−0.1	−0.2	N/A	−0.3	−0.5	N/A	0.4	N/A	0.1	0.1	N/A	N/A	0.3	0.1	N/A	N/A	N/A	N/A	−0.3	N/A	N/A
IL	LoS	ρ	−0.10	−0.12	N/A	−0.03	−0.04	−0.38	0.58	N/A	−0.34	0.17	0.03	N/A	0.42	−0.50	−0.21	N/A	N/A	N/A	−0.77	−0.29	0.52
IL	LoS	$\hat{\rho}$	−0.1	−0.1	N/A	−0.0	−0.0	−0.4	0.6	N/A	−0.3	0.2	0.0	N/A	0.4	−0.5	−0.2	N/A	N/A	N/A	−0.8	−0.3	0.5
IL	NLoS	ρ	0.08	−0.04	N/A	−0.16	0.02	N/A	0.65	N/A	−0.36	0.18	N/A	N/A	0.30	−0.34	N/A	N/A	N/A	N/A	−0.77	N/A	N/A
IL	NLoS	$\hat{\rho}$	0.1	−0.0	N/A	−0.2	0.0	N/A	0.7	N/A	−0.4	0.2	N/A	N/A	0.3	−0.3	N/A	N/A	N/A	N/A	−0.8	N/A	N/A

measurements, suburban LSP distributions of C1 were closest. This measurement, however, appears to be at minimum distance from C2-NLoS, indicating a validity of assumed macro-cell measurement setup. The proper choice of WINNER C2 parameters for representation of the whole class of urban macrocells is confirmed by the Ilmenau and Dresden measurements: these measurements are closer to the C2 reference than to each other.

For those scenarios/measurements where the correlation coefficients form a negative definite symmetric matrix, the alternating projection method is exploited to determine the closest correlation matrix. Therefore, the paper also introduces the modified WINNER scenario parameters that enable a quantification of scenario divergence.

Appendix

Parameters of WINNER Channel Model Describing MVN Distributions

In order to ensure the traceability of the presented divergences, the relevant subset of WINNER parameters is given in Tables 8 and 9. They also include the MVN distribution parameters estimated from Ilmenau and Dresden measurements. Additionally, Table 9 contains the modified correlation coefficients $\hat{\rho}$ that form positive definite correlation matrices. They are used for scenario representation instead of original coefficients.

Acknowledgment

The authors would like to acknowledge the contributions of their colleagues from EASY-C project during the conduction and analysis of measurements, especially to Carsten Jandura, Actix GmbH.

References

[1] A. F. Molisch, H. Asplund, R. Heddergott, M. Steinbauer, and T. Zwick, "The COST259 directional channel model-part I: overview and methodology," *IEEE Transactions on Wireless Communications*, vol. 5, no. 12, pp. 3421–3433, 2006.

[2] "Digital land mobile radio communications," Tech. Rep. COST207, 1989.

[3] L. Correia, Ed., *Wireless Flexible Personalised Communications: COST 259, European Co-Operation in Mobile Radio Research*, Wiley, 2001.

[4] L. Correia, "Mobile broadband multimedia networks—techniques, models and tools for 4G," Final Report COST 273, Elsevier, Oxford, UK, 2006.

[5] R. Verdone and A. Zanella, *Pervasive Mobile and Ambient Wireless Communications*, Signals and Communication Technology, Springer, London, UK, 2012.

[6] 3GPP TR25.996 V9.0.0, Spatial channel model for MIMO simulations,Third Generation Partnership Project (3GPP), Tech. Rep., December 2009, http://www.3gpp.org/.

[7] P. Kyösti, J. Meinilä, L. Hentilä et al., "IST-4-027756 WINNER II Deliverable 1.1.2. v.1.2, WINNER II Channel Models," Tech. Rep. IST-WINNERII, 2007.

[8] Guidelines for evaluation of radio interface technologies for IMTAdvanced, Report ITU-R M.2135-1, International Telecommunication Union, Radiocommunication Sector (ITU-R), 2009, http://www.itu.int/pub/R-REP-M.2135-1-.

[9] M. Narandžić, C. Schneider, and R. S. Thomä, "WINNER wideband MIMO system-level channel model, comparison with other reference models," in *Proceedings of the Internationales Wissenschartliches Kolloquium (IWK '09)*, vol. 54, Ilmenau, Germany, 2009.

[10] WINNER (Wireless world INitiative NEw Radio), http://projects.celtic-initiative.org/winner+/.

[11] M. Steinbauer, A. F. Molisch, and E. Bonek, "The double-directional radio channel," *IEEE Antennas and Propagation Magazine*, vol. 43, no. 4, pp. 51–63, 2001.

[12] "Multivariate normal distribution," http://en.wikipedia.org/wiki/Multivariate_normal_distribution.

[13] A. Gehring, M. Steinbauer, I. Gaspard, and M. Grigat, "Empirical channel stationarity in urban environments," in *Proceedings of the European Personal Mobile Communications Conference (EPMCC '01)*, Vienna, Austria, February 2001.

[14] R. Thomä, M. Landmann, and A. Richter, "RIMAX—a maximum likelihood framework for parameter estimation in multidimensional channel sounding," in *Proceedings of the International Symposium on Antennas and Propagation*, Sendai, Japan, August 2004.

[15] M. Landman, M. Narandžić, and R. S. Thomä, "Limits of experimental channel characterization related to antenna calibration," in *Proceedings of the 29th General Assembly of the International Union of Radio Science (URSI '08)*, Chicago, Ill, USA, August 2008.

[16] M. Landmann, M. Käske, and R. S. Thomä, "Impact of incomplete and inaccurate data models on high resolution parameter estimation in multidimensional channel sounding," *IEEE Transactions on Antennas and Propagation*, vol. 60, no. 2, pp. 557–573, 2012.

[17] Rusk channel sounder, http://www.channelsounder.de/.

[18] C. Schneider, M. Narandžić, M. Käske, G. Sommerkorn, and R. S. Thomä, "Large Scale parameter for the WINNER II channel model at 2. 53 GHz in urban macro cell," in *Proceedings of the IEEE 71st Vehicular Technology Conference (VTC '10)*, Taipei, Taiwan, May 2010.

[19] M. Narandžić, C. Schneider, M. Käske, S. Jäckel, G. Sommerkorn, and R. S. Thomä, "Large-scale parameters of wideband MIMO channel in urban multi-cell scenario," in *Proceedings of the 5th European Conference on Antennas and Propagation (EUCAP '11)*, pp. 3759–3763, Rome, Italy, April 2011.

[20] H. W. Lilliefors, "On the Kolmogorov-Smirnov test for normality with mean and variance unknown," *Journal of the American Statistical Association*, vol. 62, no. 318, pp. 399–402, 1967.

[21] C. M. Jarque and A. K. Bera, "A test for normality of observations and regression residuals," *International Statistical Review*, vol. 55, no. 2, pp. 163–172, 1987.

[22] S. Kullback and R. A. Leibler, "On information and sufficiency," *The Annals of Mathematical Statistics*, vol. 22, no. 1, pp. 79–86, 1951.

[23] W. D. Penny and S. J. Roberts, "Variational bayes for generalised autoregressive models," Tech. Rep. PARG-00-12, Department of Engineering Science, Oxford University, 2000.

[24] B. Fuglede and F. Topsøe, "Jensen-Shannon Divergence and Hilbert space embedding," http://www.math.ku.dk/~topsoe/ISIT2004JSD.pdf.

[25] J. P. Boyle and R. L. Dykstra, "A method for finding projections onto the intersection of convex sets in Hilbert spaces," *Advances in Order Restricted Inference*, vol. 37, pp. 28–47, 1986.

[26] N. J. Higham, "Computing the nearest correlation matrix—a problem from finance," *IMA Journal of Numerical Analysis*, vol. 22, no. 3, pp. 329–343, 2002.

[27] A. P. García Ariza, J. F. Monserrat, and L. Rubio, "Alternating projection method applied to indefinite correlation matrices for generation of synthetic MIMO channels," *International Journal of Electronics and Communications*, vol. 64, no. 1, pp. 1–7, 2010.